Plutonium(IV) Sequestration: Structural and Thermodynamic Evaluation of the Extraordinarily Stable Cerium(IV) Hydroxypyridinonate Complexes[1]

Jide Xu, Emil Radkov, Marco Ziegler, and Kenneth N. Raymond*

Department of Chemistry and Chemical Sciences Division, Lawrence Berkeley National Laboratory, University of California, Berkeley, California 94720

Received January 18, 2000

Ligands containing the 1-methyl-3-hydroxy-2(1*H*)-pyridinone group (Me-3,2-HOPO) are powerful plutonium(IV) sequestering agents. The Ce(IV) complexes of bidentate and tetradentate HOPO ligands have been quantitatively studied as models for this sequestration. The complexes $Ce(L^1)_4$, $Ce(L^2)_4$, $Ce(L^3)_2$, and $Ce(L^4)_2$ (L^1 = Me-3,2-HOPO; L^2 = PR-Me-3,2-HOPO; L^3 = 5LI-Me-3,2-HOPO; L^4 = 5LIO-Me-3,2-HOPO) were prepared in THF solution from $Ce(acac)_4$ and the corresponding ligand. The complex $Ce(L^4)_2$ was also prepared in aqueous solution by air oxidation of the Ce(III) complex $[Ce(L^4)_2]^-$. Single-crystal X-ray diffraction analyses are reported for $Ce(L^1)_4 \cdot 2CHCl_3$ [$P\bar{1}$ (no. 2), $Z = 2$, $a = 9.2604(2)$ Å, $b = 12.1992(2)$ Å, $c = 15.9400(2)$ Å, $\alpha = 73.732(1)°$, $\beta = 85.041(1)°$, $\gamma = 74.454(1)°$], $Ce(L^3)_2 \cdot 2CH_3OH$ [$P2_1/c$ (no. 14), $Z = 4$, $a = 11.7002(2)$ Å, $b = 23.0033(4)$ Å, $c = 15.7155(2)$ Å, $\beta = 96.149(1)°$], $Ce(L^4)_2 \cdot 2CH_3OH$ [$P\bar{1}$ (no. 2), $Z = 2$, $a = 11.4347(2)$ Å, $b = 13.8008(2)$ Å, $c = 15.2844(3)$ Å, $\alpha = 101.554(1)°$, $\beta = 105.691(1)°$, $\gamma = 106.746(1)°$], and $Ce(L^4)_2 \cdot 4H_2O$ [$P2_1/c$ (no. 14), $Z = 4$, $a = 11.8782(1)$ Å, $b = 22.6860(3)$ Å, $c = 15.2638(1)$ Å, $\beta = 96.956(1)°$]. A new criterion, the shape measure *S*, has been introduced to describe and compare the geometry of such complexes. It is defined as $S = \min[((1/m)\sum_{i=1}^{m}(\delta_i - \theta_i)^2)^{1/2}]$, where *m* is the number of edges, δ_i is the observed dihedral angle along the *i*th edge of δ (angle between normals of adjacent faces), θ_i is the same angle of the corresponding ideal polytopal shape θ, and min is the minimum of all possible values. For these complexes the shape measure shows that the coordination geometry is strongly influenced by small changes in the ligand backbone or solvent. Solution thermodynamic studies determined overall formation constants ($\log \beta$) for $Ce(L^2)_4$, $Ce(L^3)_2$, and $Ce(L^4)_2$ of 40.9, 41.9, and 41.6, respectively. A thermodynamic cycle has been used to calculate these values from the corresponding formation constants of Ce(III) complexes and standard electrode potentials. From the formation constants and from the protonation constants of the ligands, extraordinarily high pM values for Ce(IV) are generated by these tetradentate ligands (37.5 for $Ce(L^3)_2$ and 37.0 for $Ce(L^4)_2$). The corresponding constants for Pu(IV) are expected to be substantially the same.

Introduction

New separation technologies for the actinide elements are desirable for both chemical isolation and environmental remediation. A major project of this laboratory has been the development of specific sequestering agents for the actinides.[1−4] Ligands containing 1-hydroxy-2(1*H*)-pyridinone (1,2-HOPO) and 1-methyl-3-hydroxy-2(1*H*)-pyridinone (Me-3,2-HOPO) chelating units have been demonstrated to be effective in animals for the decorporation of Pu(IV), U(VI), Np(IV), Th(IV), and Am(III).[4−12] In such ligands (Figure 1), the HOPO groups are attached through amide linkages to suitable molecular "scaffolds". The amide link hydrogen bonds to the phenolic oxygen atoms in the HOPO anion, thereby increasing the stability of complexes formed with metals.[4] Introduction of an oxygen atom in the scaffold increases the aqueous solubility of both the ligand and its metal complexes, which is highly desirable for the design

* To whom correspondence should be addressed.

(1) This is part 44 in the series Specific Sequestering Agents for the Actinides. Part 43: Durbin, P. W.; Kullgren, B.; Xu, J.; Raymond, K. N. Chelating Agents for Uranium (VI): 2. Efficacy and Toxicity of Tetradenate Catecholate and Hydroxypyridinonate Ligands in Mice. *Health Phys.* **2000**, *78*, 511−521.

(2) Raymond, K. N.; Harris, W. R.; Carrano, C. J.; Weitl, F. L. The Synthesis, Thermodynamic Behavior, and Biological Properties of Metal-Ion-Specific Sequestering Agents for Iron and the Actinides. Reprinted from ACS Symposium Series No. 140 in *Inorganic Chemistry in Biology and Medicine*; Martell, A. E., Ed.; American Chemical Society: Washington, DC, 1980; p 313.

(3) Raymond, K. N. Specific Sequestering Agents for Iron and Actinides. In *Environmental Inorganic Chemistry;* Irgolic, K. J., Martell, A. E., Eds.; Proceedings, U.S.-Italy International Workshop on Environmental Inorganic Chemistry, San Miniato, Italy, June 5−10, 1983; VCH Publishers: Deerfield Beach, FL, 1985; p 331.

(4) Raymond, K. N.; Xu, J. Siderophore-based Hydroxypyridinone Sequestering Agents. In *The Development of Iron Chelators for Clinical Use*; Bergeron, R. G., Brittenham, G. M., Eds.; CRC Press: Boca Raton, FL, 1994; p 307.

(5) White, D. L.; Durbin, P. W.; Jeung, N.; Raymond, K. N. *J. Med. Chem.* **1988**, *31*, 11.

(6) Xu, J.; Raymond, K. N.; Durbin, P. W.; Kullgren, B. *J. Med. Chem.* **1995**, *38*, 2606.

(7) Stradling, G. N.; Gray, S. A.; Ellender, M.; Moody, J. C.; Hodgson, A.; Pearce, M.; Wilson, I.; Burgada, R.; Bailly, T. P.; Leroux, Y. G.; El Manouni, D.; Raymond, K. N.; Durbin, P. W. *Int. J. Radiat. Biol.* **1992**, *62*, 487.

(8) Volf. V.; Burgada, R.; Raymond, K. N.; Durbin, P. W. *Int. J. Radiat. Biol*. **1993**, *63*, 785.

(9) Durbin, P. W.; Kullgren, B.; Xu, J.; Raymond, K. N. *Radiat. Prot. Dosim.* **1994**, *53*, 305.

(10) Stradling, G. N.; Gray, S. A.; Pearce, M. J.; Wilson, I.; Moody, J. C.; Burgada, Durbin, P. W.; Raymond, K. N. *Hum. Exp. Toxicol*. **1995**, *14*, 165.

(11) Durbin, P. W.; Kullgren, B.; Xu, J.; Raymond, K. N.; Allen, P. G.; Bucher, J. J.; Edelstein, N. M.; Shuh, D. K. *Health Phys.* **1998**, *75*, 34.

(12) Xu, J.; Raymond, K. N. *Inorg. Chem.* **1999**, *38*, 308.

10.1021/ic000063i CCC: $19.00
Published on Web 09/05/2000

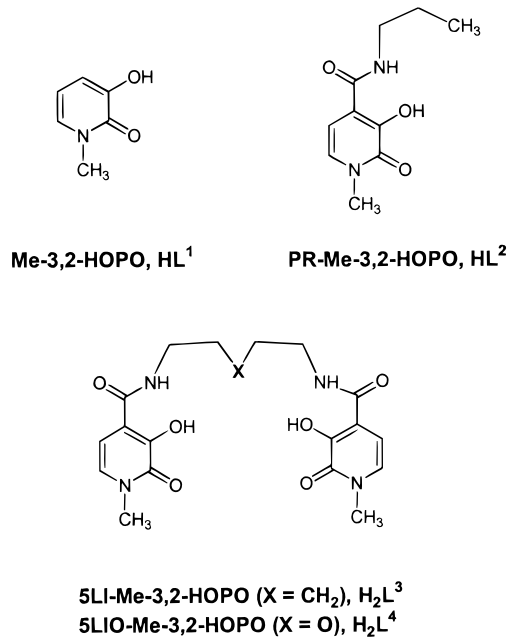

Figure 1. Bidentate and tetradentate Me-3,2-HOPO ligands reported in this paper.

of ligands for *in vivo* applications. Multidentate Me-3,2-HOPO ligands are of particular interest, because they combine low toxicity with great efficacy for *in vivo* chelation of Pu(IV).[6] Tetradentate, hexadentate, and octadentate ligands based on the Me-3,2-HOPO group are highly, and almost equally, effective when injected.[6] Remarkably, the octadentate Me-3,2-HOPO ligands are also highly effective when orally administered. The correlation of structure, biological activity, and thermodynamic stability of these complexes is an essential part of their characterization as sequestering agents.

The aqueous coordination chemistry of Ce(IV) with catechols parallels that of Pu(IV), giving the same shift in the IV/III redox potentials.[13,14] The ion size of Ce(IV) is the same as that of Pu(IV) (0.94 Å).[15] Therefore, the investigation of the Ce(IV) complexation of the HOPO ligands provides a preliminary evaluation of the Pu(IV) complexation. Ligands such as catechols, which coordinate selectively to Ce(IV), lower the reduction potential and stabilize the Ce(IV) complexes, provided that the pH is sufficiently high to fully deprotonate the ligand. The bidentate HOPO monoanions are isoelectronic with the catecholate dianion and display similar complexation behavior. However, HOPO analogues are more acidic and become effective for chelation at lower pH than catechol ligands. Here, we examine the preparation, structures, and stability of Ce(IV) complexes with the bi- and tetradentate Me-3,2-HOPO ligands and evaluate the effect of higher ligand denticity in Ce(IV) complexes with Me-3,2-HOPO ligands. Additionally, we introduce a new quantitative criterion, the *shape measure*, to evaluate and compare the coordination polyhedra in such eight-coordinate Ce(IV) complexes.

Experimental Section

All chemicals were used as received from Aldrich unless otherwise noted. ^{1}H NMR and ^{13}C NMR spectra were obtained on a Bruker AMX-300 or DRX-500 spectrometer and are reported in parts per million. The bidentate ligands Me-3,2-HOPO (HL^1) and PR-Me-3,2-HOPO (HL^2) and tetradentate 5LI-Me-3,2-HOPO (H_2L^3) and 5LIO-Me-3,2-HOPO (H_2L^4) were synthesized using published procedures.[1,6] $Ce(acac)_4$ was prepared from $Ce(acac)_3 \cdot 3H_2O$.[16,17] The potentiometry and cyclic voltametry experiments were performed at 25 °C and an ionic strength of 0.1 M. The elemental (CHN) analyses were performed at the Elemental Analysis Facility, College of Chemistry, University of California, Berkeley.

Syntheses. $[Ce(L^1)_4]\cdot 2CHCl_3$. A solution of $Ce(acac)_4$ (54 mg, 0.10 mmol) in THF (20 mL) was added slowly to a stirred solution of Me-3,2-HOPO (54 mg, 0 42 mmol) in THF (20 mL). The resultant deep brown solution was stirred under N_2 for 3 h and evaporated to dryness. More THF (30 mL) was added, and the mixture was heated at reflux overnight. The solvent was removed under vacuum, and the residue was dissolved in chloroform (15 mL), and exposed to ether vapor. After several days, the pure complex was obtained as blue-black crystals (yield 52.5 mg, 82% based on $Ce(acac)_4$). ^{1}H NMR (300 MHz, $CDCl_3$): δ 3.70 (s, 12H, CH_3), 6.13 (d, $J = 7.2$ Hz, 4H, arom H), 6.23 (t, $J = 7.2$ Hz, 4H, arom H), 6.47 (d, $J = 7.2$ Hz, 4H, arom H). Anal. Calcd (Found) for $CeC_{24}H_{24}N_4O_8\cdot 2CHCl_3$ (875.38): C, 35.67 (35.42); H, 2.99 (2.85); N, 6.40 (6.27).

$[Ce(L^2)_4]\cdot 2H_2O$. A solution of $Ce(acac)_4$ (27 mg, 0.05 mmol) in THF (10 mL) was added slowly to a stirred solution of PR-Me-3,2-HOPO (47 mg, 0.21 mmol) in THF (15 mL). The resultant blue-purple solution was stirred under N_2 and evaporated to dryness. After the addition of more THF (30 mL), the mixture was heated at reflux overnight. The solvent was removed under vacuum, and the residue was purified on a Sephadex LH20 column using methanol as eluent, yielding a blue-black powder (32 mg, 61% based on $Ce(acac)_4$). ^{1}H NMR (300 MHz, $CDCl_3$): δ 0.95 (t, $J = 7.5$ Hz, 12H, CH_3), 1.43 (q, $J = 7.3$ Hz, 8 H, CH_2), 3.33 (q, $J = 7.3$ Hz, 8H, CH_2), 3.58 (s, 12H, CH_3), 6.63 (d, $J = 6.9$ Hz, 4H, arom H), 7.16 (d, $J = 6.9$ Hz, 4H, arom H), 9.06 (s, 4H, amide H). Anal. Calcd (Found) for $CeC_{40}H_{52}N_8O_{12}\cdot 2H_2O$ (1013.06): C, 47.42 (47.27); H, 5.57 (5.84); N, 11.06 (10.87).

$[Ce(L^3)_2]\cdot 2H_2O$. To a warm (60 °C) stirred suspension of 5LI-Me-3,2-HOPO (92 mg, 0.22 mmol) in THF (25 mL) was added slowly a solution of $Ce(acac)_4$ (54 mg, 0.1 mmol) in THF (10 mL). The reaction mixture was heated at reflux under nitrogen overnight. The blue-black precipitate was collected by filtration, dissolved in chloroform, and purified by a flash silica column with 2−5% methanol in methylene chloride, to obtain a blue-black solid as the product (75 mg, 77% based on $Ce(acac)_4$). ^{1}H NMR (300 MHz, $CDCl_3$): δ 1.60 (s, 8H, CH_2), 1.75 (s, 4H, CH_2), 3.15 (s, 4H, CH_2), 3.59 (s, 12H, CH_3), 3.78 (s, 4H, CH_2), 6.64 (d, $J = 7.0$ Hz, 4H, arom H), 7.19 (d, $J = 7.0$ Hz, 4H, arom H), 9.34 (s, 4H, amide H). ^{13}C NMR (500 MHz, $CDCl_3$): δ 24.7, 28.5, 37.8, 38.9, 111.1, 117.2, 122.4, 158.3, 163.9, 164.9. Anal. Calcd (Found) for $CeC_{38}H_{44}N_8O_{12}\cdot 2H_2O$ (980.978): C, 46.52 (46.31); H, 4.93 (5.05); N 11.42 (11.13).

$[Ce(L^4)_2]\cdot 4H_2O$. This preparation followed that of Ce-5LI-Me-3,2-HOPO, except that 5LIO-Me-3,2-HOPO (93 mg, 0.22 mmol) was used. Separation and purification were performed as for Ce-5LI-Me-3,2-HOPO. Yield: 81 mg, 83% based on $Ce(acac)_4$. ^{1}H NMR (300 MHz, $CDCl_3$): δ 1.79 (s, 8H, CH_2), 3.54 (s, 8H, CH_2), 3.65 (s, 12H, CH_3), 6.61 (d, $J = 7.2$ Hz, 4H, arom H), 7.13 (d, $J = 7.2$ Hz, 4H, arom H), 9.58 (s, 4H, amide H). ^{13}C NMR (500 MHz, $CDCl_3$): δ 37.8, 39.2, 70.5, 111.1, 116.6, 122.0, 156.3, 164.0, 165.0. Anal. Calcd (Found) for $CeC_{36}H_{40}N_8O_{14}\cdot 4H_2O$ (1020.95): C, 42.35 (42.51); H, 4.73 (4.79); N, 10.97 (10.78).

An alternative synthesis of this compound proceeded from the oxidation of $[Ce(III)(L^4)_2]^-$ in aqueous solution by atmospheric oxygen. Dark purple crystals deposited from the solution over several weeks. This crystalline product has an NMR spectrum identical to that prepared from nonaqueous solution.

X-ray Crystallography. Blue-black rhomboid crystals of $[Ce(L^1)_4]\cdot 2CHCl_3$, $[Ce(L^3)_2]\cdot 2CH_3OH$, and $[Ce(L^4)_2]\cdot 2CH_3OH$ were grown by diffusing ethyl ether into a solution of the complex in a chloroform−methanol mixture. Blue-black rhomboid crystals of $[Ce(L^4)_2]\cdot 4H_2O$ were

(13) Kappel, M. J. Ph.D. Thesis, University of California, Berkeley, 1983, Chapter IV.
(14) Kappel, M. J.; Nitsche, H.; Raymond, K. N. *Inorg. Chem.* **1984**, *24*, 605.
(15) Shannon, R. D.; Prewitt, C. T. *Acta Crystallogr.* **1969**, *B25*, 925.
(16) *Gmelin Handbuch der Anorganischen Chemie*, 8th ed.; Springer: Berlin, 1980; Syst. No. 39, Rare Earth Elements, Part D2, p 100.
(17) Titze, H. *Acta Chem. Scand.* **1969**, *23*, 399.

Table 1. X-ray Crystallographic Information for $[Ce(IV)(L^1)_4]$, $[Ce(IV)(L^3)_2]\cdot 2CH_3OH$, $[Ce(IV)(L^4)_2]\cdot 2CH_3OH$, and $[Ce(IV)(L^4)_2]\cdot 4H_2O$

	$[Ce(IV)(L^1)_4]\cdot 2CHCl_3$	$[Ce(IV)(L^3)_2]\cdot 2CH_3OH$	$[Ce(IV)(L^4)_2]\cdot 2CH_3OH$[a]	$[Ce(IV)(L^4)_2]\cdot 4H_2O$[b]
empirical formula	$CeC_{26}H_{26}N_4O_8Cl_6$	$CeC_{40}H_{52}N_8O_{14}$	$CeC_{38}H_{48}N_8O_{16}$	$CeC_{36}H_{48}N_8O_{18}$
fw	875.38	1009.03	1012.97	1020.95
space group	$P\bar{1}$ (no. 2)	$P2_1/c$ (no. 14)	$P\bar{1}$ (no. 2)	$P2_1/c$ (no. 14)
T, °C	−107 (2)	−112 (1)	−112 (1)	−128(2)
λ, Å	0.710 72	0.710 72	0.710 72	0.710 72
a, Å	9.2604(2)	11.7002(2)	11.4347(2)	11.8782(1)
b, Å	12.1992(2)	23.0033(4)	13.8008(2)	22.6860(3)
c, Å	15.9400(2)	15.7155(2)	15.2844(3)	15.2638(1)
α, deg	73.732(1)	90	101.554(1)	90
β, deg	85.041(1)	96.149(1)	105.691(1)	96.956(1)
γ, deg	74.454(1)	90	106.746(1)	90
V, Å^3	1665.27(5)	4205.38(10)	2119.96(7)	4082.84(6)
Z	2	4	2	4
ρ_{calcd}, g·cm^{-3}	1.841	1.492	1.735	1.452
μ, cm^{-1}	19.05	11.52	12.88	11.90
transm coeff	0.827−0.592	0.933−0.789	0.931−0.793	0.812−0.687
R[c] $[I > 3\sigma(I)]$	0.047	0.033	0.038	0.022
R_w[d] $[I > 3\sigma(I)]$	0.053	0.036	0.049	0.031

[a] Synthesized and crystallized from a nonaqueous medium. [b] Synthesized and crystallized from an aqueous medium. [c] $R = \sum||F_o| - |F_c||/\sum|F_o|$. [d] $R_w = [(\sum w(|F_o| - |F_c|)^2/\sum wF_o^2)]^{1/2}$.

grown by atmospheric oxidation of $[Ce(III)(L^4)_2]^-$ in aqueous solution at room temperature over weeks. Selected crystals were mounted in Paratone N oil on the ends of quartz capillaries and frozen into place under a low-temperature nitrogen stream. Data were collected on a Siemens SMART/CCD X-ray diffractometer[18] with Mo Kα radiation ($\lambda = 0.710\ 72$ Å). The intensity data to a maximum 2θ range of 52.00−52.16° were extracted from the frames using the program SAINT[19] with box parameters of 1.6 × 1.6 × 0.6. The data were corrected for Lorentz and polarization effects, and an empirical absorption correction was applied using the SADABS[20] program. No decay correction was applied. The structures were solved by direct methods (Texsan)[21] and refined on F using full-matrix least-squares. All non-hydrogen atoms were refined anisotropically. Hydrogen atoms were assigned to idealized positions. Crystallographic information is summarized in Table 1.

Potentiometric Titrations. Potentiometric titrations were carried out at 25 °C under Ar in 0.1 M KCl solutions prepared with deionized and degassed water. The apparatus and method used have been previously described.[22] Unless otherwise specified, the initial volume of supporting electrolyte was 50 mL, and solid ligands, $CeCl_3$ stock solutions, or other reagents were added as necessary.

The Ce(III) complexes were studied using metal-to-ligand ratios ranging from 1:1 to 1:4, with total amounts of Ce(III) between 0.01 and 0.1 mmol. In a typical experiment the ligand was dissolved first, followed by addition of a measured amount of the $CeCl_3$ stock solution and 1−2 mL of 0.1 M HCl, to give an initial pH of approximately 2.4.

The Ce(III)−5LI-Me-3,2-HOPO system presented a difficulty due to the low solubility of the ligand in water. To overcome this problem, a measured amount of ligand (0.01−0.04 mmol) was first suspended in 50 or 100 mL of 0.1 M KCl. The required volume of $CeCl_3$ stock solution was then added, dissolving most of the ligand. The pH of the mixture was raised carefully by slow addition of small amounts of 0.1 M KOH. After all of the ligand dissolved, the titrations were carried out either from high to low pH with 0.1 M HCl or in the opposite direction with 0.1 M KOH after the lowest pH (2.3−2.5) was reached, according to the previous method.

Spectrophotometric Titrations. Spectrophotometric titrations were performed at 25 °C in 0.1 M KCl under N_2 using an HP-8452 spectrophotometer under computer control.[23] A total of 10 titrations were carried out with solutions of the $[Ce(L^4)_2]$ complex, either by addition of 0.1 M KOH or by back-titration with 0.1 M HCl. The absorbance data were processed with the least-squares program REFSPEC.[23]

Electrochemical Measurements. A BAS100A electrochemical analyzer was used for the cyclic voltammetry (CV) experiments. For aqueous solutions the supporting electrolyte was 0.1 M KCl; for acetonitrile solutions it was 0.1 M tetrabutylammonium hexafluorophosphate. The working electrode was glassy carbon or smooth Pt or Au (BAS), and the reference electrode was a AgCl/Ag electrode for an aqueous medium or 0.1 M $AgNO_3$/Ag for an acetonitrile medium; the counter electrode was a Pt wire.

Static Potentiometry. Potentiometry experiments were performed in the titration cell. A piece of Teflon tubing was used to pass a continuous flow of argon through the solution, and a combination redox electrode (Pt−AgCl/Ag from Corning) was employed for the measurements. Pure Ce(IV) complexes were used in the static potentiometric measurements as freshly prepared solutions in 0.1 M KCl. These were added in portions to fixed amounts of their Ce(III) counterparts, prepared also in 0.1 M KCl by mixing the $CeCl_3$ stock solution with a stoichiometric quantity of the ligand followed by neutralization with 0.1 M KOH. The voltage was recorded after each addition at 5 min intervals until the difference between two consecutive readings was no greater than 0.2 mV. In the cases where less than 1 μmol of a Ce(III) complex was prepared, voltage readings were taken at shorter intervals (1−2 min), due to a noticeable downward drift over extended periods of time. Each addition of Ce(IV) complex was performed under argon in less than 20 s, to prevent air oxidation of the Ce(III) complex. Similar experiments were carried out with solutions of 1−2 mmol of Ce(IV) complexes dissolved in DMF (0.200 mL) by adding suitably scaled aliquots of the corresponding Ce(III) complexes.

Results and Discussion

The Shape Measure. Eight-coordinate complexes are known in a variety of coordination geometries for which the assignment to the closest idealized polyhedron usually is not straightforward. An analysis of the shape is usually expressed in terms of three high-symmetry polyhedra (Figure 2): the trigonal dodecahedron, the bicapped trigonal prism, and the square antiprism.[24−26] Following Porai-Koshits and Aslanov,[26] an approach was

(18) SMART Area Detector Software Package, Siemens Industrial Automation, Inc., Madison, WI, 1995.
(19) SAINT: SAX Area-Detector Integration Program (V.4.024), Siemens Industrial Automation, Inc., Madison, WI, 1995.
(20) Sheldrick, G. SADABS: Siemens Area Detector ABSsorption correction program, advance copy, private communication, 1996.
(21) TeXsan: Crystal Structure Analysis Package, Molecular Structure Corp., 1985, 1992.
(22) Harris, W. R.; Raymond, K. N. *J. Am. Chem. Soc.* **1979**, *101*, 6534.
(23) Turowski, P. N.; Rodgers, S. J.; Scarrow, R. C.; Raymond, K. N. *Inorg. Chem.* **1988**, *27*, 474.
(24) Hoard, J. L.; Silverton, J. V. *Inorg. Chem.* **1963**, *2*, 235−250.
(25) Lippard, S. J.; Russ, B. J. *Inorg. Chem.* **1968**, *7*, 1686.
(26) Porai-Koshits, M. A.; Aslanov, L. A. *Russ. J. Struct. Chem.* **1974**, *13*, 244.

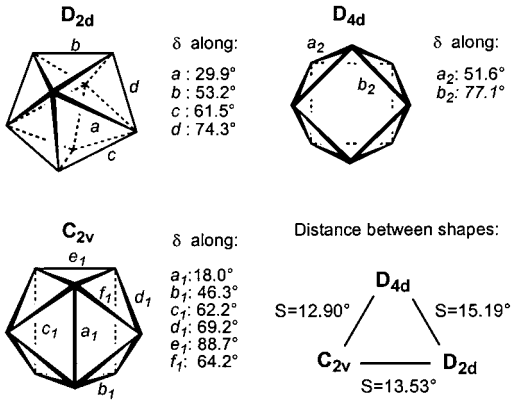

Figure 2. Geometries of the three idealized eight-coordinate polyhedra (trigonal dodecahedron (D_{2d}), bicapped trigonal prism (C_{2v}), and square antiprism (D_{4d}) with shape measure S (deg) given for each pair.

suggested by Muetterties and Guggenberger[27] for determining the polyhedral shape by comparing chosen ideal and observed pertinent dihedral angles and the nonplanarity of the trapezoidal-type atoms. Ideal coordination geometries were in turn proposed by Kepert,[28,29] taking into account a repulsive potential of the form ($\sum_{i\neq j}^{m} R_{ij}^{-n}$) to optimize the ideal coordination geometry of a given symmetry. We will refer to this as the Kepert model, and have chosen $n = 8$. Dihedral angles along edges are defined as the angles between the normals to adjacent binding faces of the polyhedron, where the vertices of that polyhedron are the ligand donor atoms around the metal. This "shape analysis" is then independent of the size of the polyhedron, allowing for the comparison of complexes formed by various metal ions and ligands. Another approach is to fit (in a least-squares sense) all the vertices of the observed polyhedron to that of idealized values, which was recently proposed as a continuous symmetry measure.[30]

We have chosen to compare the dihedral angles, since these are intrinsically connected with the notion of shape, i.e., the symmetry. In previous approaches to shape analysis,[24−29] only specific dihedral angles were used. If the symmetry of the complex deviates significantly from an idealized geometry, it is difficult, however, to decide which dihedral angles to choose. We therefore suggest that the geometry of complexes be analyzed using *all* the dihedral angles (one for each pair of adjacent triangular planes) in the polyhedron. All observed dihedral angles in a given structure could then be compared with the corresponding ideal values. To that end, following general error theory, we suggest the use of S, the "shape measure", to evaluate the degree of distortion from an ideal geometry; S is the minimal variance of dihedral angles along all edges defined as

$$S(\delta,\theta) = \min[((1/m)\sum_{i=1}^{m}(\delta_i - \theta_i)^2)^{1/2}] \qquad (1)$$

where m is the number of all possible edges (here $m = 18$). δ_i is the observed dihedral angle (angle between normals of adjacent faces) along the ith edge of the experimental polyhedron δ, and θ_i is the same angle of the corresponding ideal polytopal shape θ (D_{2d}, D_{4d}, or C_{2v} structures shown in Figure 2).[29] The minimization is carried out by looking at all possible orientations of the observed structure (δ) relative to the reference polyhedron (θ). The value $S(\delta,\theta)$ is a measure (a metric in the strict mathematical sense) of structural resemblance to an ideal polytopal shape.

The shape analysis of a coordination polyhedron is performed in three steps. The first step is the calculation of all the dihedral angles of each pair of adjacent planes in the polyhedron. The second step in this analysis is to find which superposition of the polyhedron on the targeted ideal polyhedron gives the smallest deviation for that idealized shape. Finally, eq 1 is used to compare S for the different ideal coordination geometries. A computer program that incorporates this algorithm has been developed (Table S-VI in the Supporting Information). The shape measures for the idealized polytopal shapes are depicted in Figure 2.

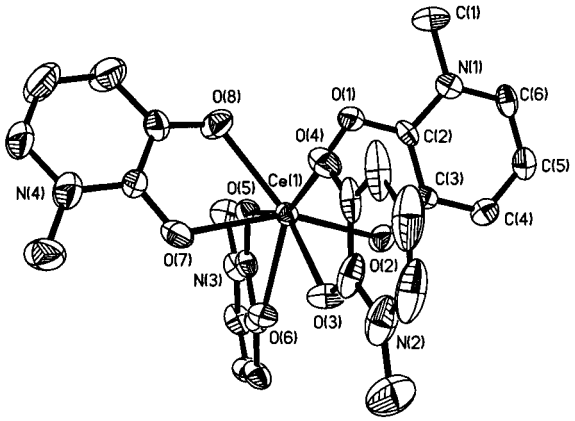

Figure 3. Crystal structure of $[Ce(IV)(L^1)_4]\cdot 2CHCl_3$ (ORTEP). Thermal ellipsoids are drawn at the 50% probability level.

Table 2. Selected Bond Lengths (Å) and Bond Angles (deg) for $[Ce(IV)(L^1)_4]\cdot 2CHCl_3$

Bond Lengths			
Ce(1)−O(1)	2.470(6)	Ce(1)−O(2)	2.253(5)
Ce(1)−O(3)	2.401(5)	Ce(1)−O(4)	2.310(6)
Ce(1)−O(5)	2.386(5)	Ce(1)−O(6)	2.288(6)
Ce(1)−O(7)	2.462(6)	Ce(1)−O(8)	2.306(6)
Bond Angles			
O(1)−Ce(1)−O(2)	65.9(2)	O(1)−Ce(1)−O(8)	73.0(2)
O(3)−Ce(1)−O(4)	66.5(2)	O(2)−Ce(1)−O(7)	157.3(2)
O(5)−Ce(1)−O(6)	67.5(2)	O(3)−Ce(1)−O(6)	72.3(2)
O(7)−Ce(1)−O(8)	65.8(2)	O(4)−Ce(1)−O(5)	154.1(2)
O(1)−Ce(1)−O(4)	74.6(2)	O(5)−Ce(1)−O(8)	77.6(2)
O(1)−Ce(1)−O(5)	85.0(2)	O(4)−Ce(1)−O(8)	81.2(2)
O(2)−Ce(1)−O(3)	81.7(2)	O(3)−Ce(1)−O(7)	80.9(2)
O(2)−Ce(1)−O(6)	80.5(2)	O(6)−Ce(1)−O(7)	80.4(2)

Structures of the Ce(IV) Complexes with Me-3,2-HOPO Ligands. Ce(IV)−Tetrakis(Me-3,2-HOPO) Complex, $[Ce(L^1)_4]\cdot 2CHCl_3$. This complex crystallizes in the triclinic space group $P\bar{1}$ (no. 2) with $Z = 2$; there are two independent complex molecules and four chloroform molecules (two are disordered) in each unit cell. The structure of $[Ce(L^1)_4]$ is shown in Figure 3, and selected bond lengths and angles are given in Table 2. The following shape measures were obtained:

$$S(D_{2d}) = 13.6°; \quad S(C_{2v}) = 14.6°; \quad S(D_{4d}) = 16.8°$$

The above values of S show that the coordination geometry deviates significantly from an ideal polyhedron, and resembles best a trigonal dodecahedron. The cerium atom is coplanar with the HOPO oxygens of each pair of Me-3,2-HOPOs (mean

(27) Muetteries, E. L.; Guggenberger, L. J. *J. Am. Chem. Soc*. **1974**, *96*, 1748.
(28) Kepert, D. L. Aspects of the Stereochemistry of Six-Coordination. *Prog. Inorg. Chem*. **1977**, *23*, 1.
(29) Kepert, D. L. Aspects of the Stereochemistry of Eight-Coordination. *Prog. Inorg. Chem*. **1978**, *24*, 179.
(30) Pinsky, M.; Avnir, D. *Inorg. Chem*. **1998**, *37*, 5575.

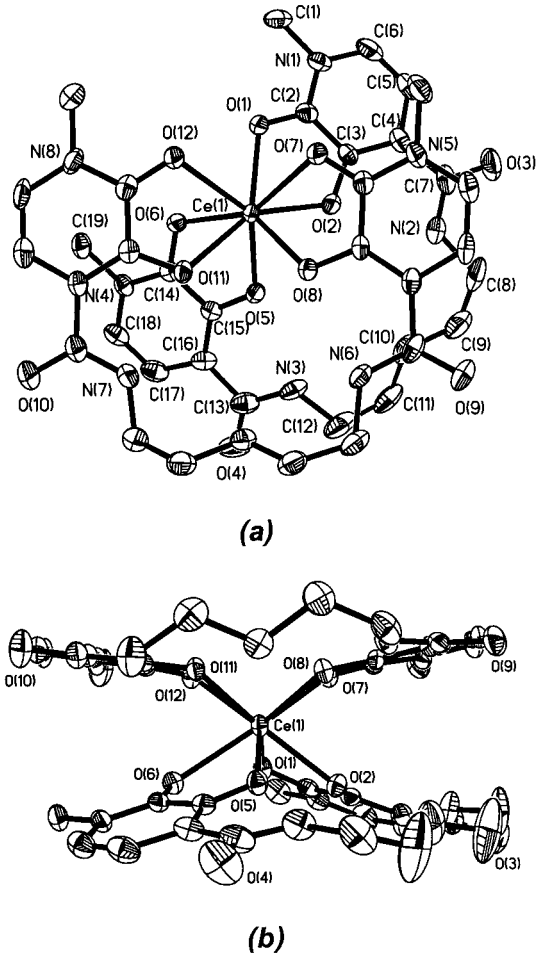

Figure 4. Crystal structure (ORTEP) of $[Ce(IV)(L^3)_2]\cdot 2CH_3OH$: (a) top view; (b) side view. Thermal ellipsoids are drawn at the 50% probability level.

deviations from the least-squares planes are 0.16 and 0.08 Å, respectively). The two least-squares planes are essentially perpendicular, forming a dihedral angle of 88.1°. All HOPO rings are planar with mean deviations from the least-squares plane within the range of 0.004−0.015 Å. However, each HOPO ring plane is slightly bent toward its attached chelate plane, composed of the central cerium and HOPO oxygen atoms; the average angle is 7.5°. The average $Ce-O_{phen}$ length (2.29(3) Å) is much shorter than that of $Ce-O_{oxo}$ (2.43(4) Å), as expected from the charge distribution.

Ce(IV)−Bis(5LI-Me-3,2-HOPO) Complex, $[Ce(L^3)_2]\cdot 2CH_3OH$. This compound crystallizes in the monoclinic space group $P2_1/c$ with $Z = 4$. Each asymmetric unit contains one complex and two highly disordered methanol molecules. The structure is shown in Figure 4; the selected bond lengths and angles are given in Table 3. The cerium atom is coordinated by eight oxygen atoms of the two 5LI-Me-3,2-HOPO ligands in a slightly distorted square antiprism geometry with a sandwich-like shape (Figure 4b); the square faces of the "top" and "bottom" ligands are offset and rotated about 45° relative to one another (Figure 4a). The HOPO ring planes are bent, with their attached chelate planes forming an average angle of 24.6°. As a result, the top and bottom ligands are close to each other (Figure 4b), with the nearest vertical distance between the HOPO rings of top and bottom ligands about 4 Å (significantly larger than the 3.4 Å of aromatic ring π-stacking[31]). The geometry of the coordination polyhedron in $[Ce(IV)(L^3)_2]\cdot 2CH_3OH$ approaches a "regular" square antiprism

Table 3. Selected Bond Lengths (Å) and Bond Angles (deg) for $[Ce(IV)(L^3)_2]\cdot 2CH_3OH$

Bond Lengths			
Ce(1)−O(1)	2.378(3)	Ce(1)−O(2)	2.303(3)
Ce(1)−O(6)	2.408(3)	Ce(1)−O(5)	2.301(3)
Ce(1)−O(7)	2.426(3)	Ce(1)−O(8)	2.291(3)
Ce(1)−O(12)	2.397(3)	Ce(1)−O(11)	2.333(3)
Bond Angles			
O(1)−Ce(1)−O(2)	67.6(1)	O(1)−Ce(1)−O(5)	120.8(1)
O(5)−Ce(1)−O(6)	67.3(1)	O(2)−Ce(1)−O(6)	109.0(1)
O(7)−Ce(1)−O(8)	67.2(1)	O(7)−Ce(1)−O(11)	117.3(1)
O(11)−Ce(1)−O(12)	67.0(1)	O(8)−Ce(1)−O(12)	117.5(1)
O(1)−Ce(1)−O(7)	73.4(1)	O(2)−Ce(1)−O(7)	73.5(1)
O(1)−Ce(1)−O(12)	76.8(1)	O(2)−Ce(1)−O(8)	83.5(1)
O(5)−Ce(1)−O(8)	80.0(1)	O(6)−Ce(1)−O(11)	74.8(1)
O(5)−Ce(1)−O(11)	78.6(1)	O(6)−Ce(1)−O(12)	75.5(1)

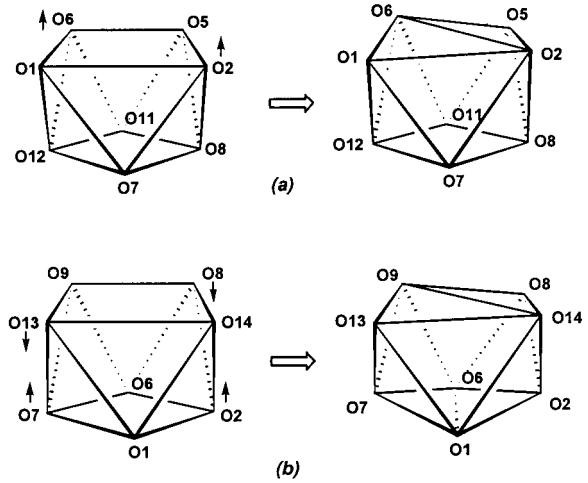

Figure 5. Possible distortion pathways of the coordination polyhedra from the ideal D_{4d} square antiprism: (a) $[Ce(IV)(L^3)_2]\cdot 2CH_3OH$; (b) $[Ce(IV)(L^4)_2]\cdot 2CH_3OH$.

(Figure 4a). Least-squares analysis shows that its top and bottom square planes are tilted by 4.7° and that the atoms deviate about 0.1 Å from the idealized planes. The dihedral angles in a regular square antiprism (Kepert model, $n = 8$) are 77.1° and 51.6° for the square−triangle (ST) dihedral angle and the triangle−triangle (TT) dihedral angle, respectively. The following values of S are found for the D_{2d} trigonal dodecahedron, the C_{2v} bicapped trigonal prism, and the D_{4d} square antiprism (the symbols in parentheses indicate the corresponding ideal shapes):

$$S(D_{2d}) = 20.7°; \quad S(C_{2v}) = 18.2°; \quad S(D_{4d}) = 12.7°$$

The lower shape measure for the D_{4d} comparison indicates that the coordination polyhedron is closest to an idealized square antiprism. Careful examination of the structure of $[Ce(IV)(L^3)_2]\cdot 2CH_3OH$ shows that the top square plane O(1)O(2)O(5)O(6) is slightly bent, such that the plane O(1)O(2)O(6) forms a 12.1° dihedral angle with the plane O(2)O(5)O(6) while the plane O(1)O(2)O(6) forms a 72.0° dihedral angle with the plane O(1)O(2)O(7), and a 66.1° dihedral angle with the plane O(1)O(6)O(12) (Figure 5a). Both of these dihedral angles are smaller than the 77.1° value for the ideal D_{4d} geometry because atoms O(2) and O(6) are above the top least-squares plane of the polyhedron, as shown in Figure 4a.

The average $Ce-O_{phen}$ and $Ce-O_{oxo}$ lengths are 2.30(5) and 2.40(6) Å, respectively. The difference of $Ce-O_{phen}$ and $Ce-O_{oxo}$ in this complex (0.09(3) Å) is smaller than that of the

(31) Hunter, C. A.; Sanders, J. K. *J. Am. Chem. Soc.* **1990**, *112*, 5525.

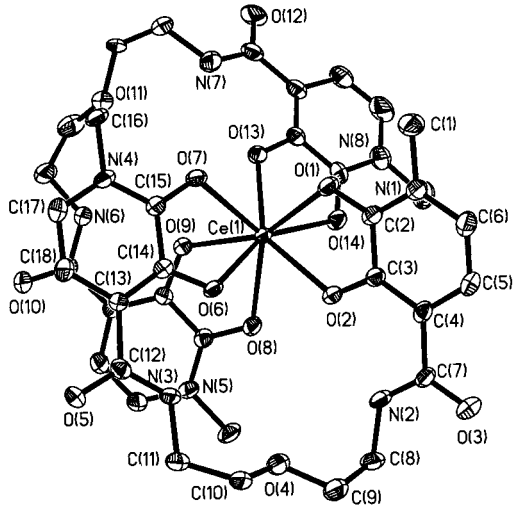

Figure 6. Crystal structure (ORTEP) of $[Ce(IV)(L^4)_2]\cdot 2CH_3OH$. Thermal ellipsoids are drawn at the 50% probability level.

Table 4. Selected Bond Lengths (Å) and Bond Angles (deg) for $[Ce(IV)(L^4)_2]\cdot 2CH_3OH$

Bond Lengths			
Ce(1)−O(1)	2.395(3)	Ce(1)−O(2)	2.290(3)
Ce(1)−O(7)	2.387(3)	Ce(1)−O(6)	2.308(3)
Ce(1)−O(8)	2.424(3)	Ce(1)−O(9)	2.305(3)
Ce(1)−O(14)	2.422(3)	Ce(1)−O(13)	2.281(3)
Bond Angles			
O(1)−Ce(1)−O(2)	67.21(10)	O(1)−Ce(1)−O(7)	80.29(10)
O(6)−Ce(1)−O(7)	67.33(9)	O(2)−Ce(1)−O(6)	78.22(10)
O(8)−Ce(1)−O(9)	66.48(10)	O(8)−Ce(1)−O(14)	88.6(1)
O(13)−Ce(1)−O(14)	66.91(10)	O(9)−Ce(1)−O(13)	78.7(1)
O(1)−Ce(1)−O(14)	79.8(1)	O(1)−Ce(1)−O(6)	97.8(1)
O(2)−Ce(1)−O(8)	71.14(10)	O(2)−Ce(1)−O(7)	128.3(1)
O(6)−Ce(1)−O(9)	81.7(1)	O(8)−Ce(1)−O(13)	126.1(1)
O(7)−Ce(1)−O(13)	73.58(10)	O(9)−Ce(1)−O(14)	111.5(1)

complex of unsubstituted Me-3,2-HOPO $[Ce(IV)(L^1)_4]$ (0.14(4) Å) due to the delocalization caused by the carboxamide group of the 5LI-Me-3,2-HOPO moiety. The distances between the amide nitrogen and its adjacent phenolic oxygen atoms are 2.689(5)−2.718(5) Å, due to the strong hydrogen bonding that contributes to the stabilization of the complex.[32]

Ce(IV)−Bis(5LIO-Me-3,2-HOPO) Complex, $[Ce(L^4)_2]\cdot 2CH_3OH$. The complex crystallizes in $P\bar{1}$ (no. 2) with $Z = 2$; each asymmetric unit contains one metal complex and two methanol molecules. The oxygen O(15) of the methanol molecules hydrogen bonds with the amide oxygens O(5) of the complex with a distance of 2.72(1) Å. The other methanol molecule is highly disordered. The structure of $[Ce(L^4)_2]\cdot 2CH_3OH$ is slightly disordered; the ethylene bridge between N(7) and O(11) is disordered and can be modeled over two sites with an occupation of 0.6055 and 0.3945. This minor disorder should not affect the coordination geometry significantly and will not be discussed in the text. The structure is shown in Figure 6 (the disordered ethylene and solvents are not shown), and selected bond lengths and angles are given in Table 4. The central atom is coordinated by eight oxygen atoms of the two 5LIO-Me-3,2-HOPO ligands, and the complex also has a sandwich-like shape similar to that of $[Ce(L^3)_2]\cdot 2CH_3OH$. The HOPO ring planes are bent with their attached chelate planes defined by the cerium and HOPO oxygen atoms, forming an average dihedral angle of 13.3°, much less than that of $[Ce(L^3)_2]\cdot 2CH_3OH$. The coordination polyhedron of $[Ce(IV)(L^4)_2]\cdot 2CH_3OH$ could be considered as a highly distorted square antiprism, in which the oxygen donor atoms deviate from the least-squares planes by 0.1−0.3 Å. The top and bottom square planes are bent as shown in Figure 5b. The planes O(1)O(2)O(6) and O(1)O(6)O(7) form a 22.7° dihedral angle, and the plane O(8)O(9)O(14) forms a 15.0° dihedral angle with the plane O(9)O(13)O(14). This distortion is toward a triangular dodecahedron. On the basis of the same shape analysis of all dihedral angles in this complex, the calculated shape measures for different polyhedron geometries are

$$S(D_{2d}) = 14.3°; \quad S(C_{2v}) = 14.9°; \quad S(D_{4d}) = 17.8°$$

Since these three values are similar, this structure cannot be described in terms of an idealized geometry.

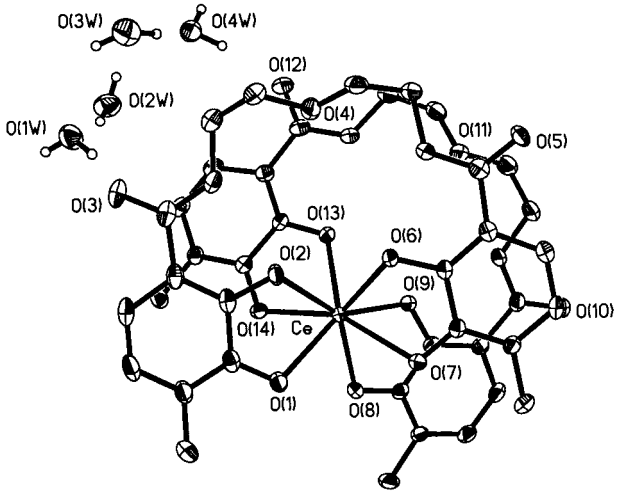

Figure 7. Crystal structure (ORTEP) of $[Ce(IV)(L^4)_2]\cdot 4H_2O$ from an aqueous medium. Thermal ellipsoids are drawn at the 50% probability level. Distance (Å): O(1W)- - -O(3) (amide oxygen), 2.743(3); O(1W)- - -O(10) (amide oxygen of another complex), 2.848(4); O(1W)- - -O(2W), 2.882(4); O(1W)- - -O(3W), 2.934(4); O(2W)- - -O(3W), 3.377(4); O(4W)- - -O(12) (amide oxygen), 2.795(3); O(4W)- - -O(5) (amide oxygen of another complex), 2.805(4).

Table 5. Selected Bond Lengths (Å) and Bond Angles (degree) for $[Ce(IV)(L^4)_2]\cdot 4H_2O$

Bond Lengths			
Ce(1)−O(1)	2.414(2)	Ce(1)−O(2)	2.313(2)
Ce(1)−O(7)	2.431(2)	Ce(1)−O(6)	2.277(2)
Ce(1)−O(8)	2.387(2)	Ce(1)−O(9)	2.292(2)
Ce(1)−O(14)	2.405(2)	Ce(1)−O(13)	2.291(2)
Bond Angles			
O(1)−Ce(1)−O(2)	66.96(7)	O(1)−Ce(1)−O(7)	88.45(6)
O(6)−Ce(1)−O(7)	67.22(6)	O(2)−Ce(1)−O(6)	74.15(6)
O(8)−Ce(1)−O(9)	67.74(6)	O(8)−Ce(1)−O(14)	83.97(6)
O(13)−Ce(1)−O(14)	67.33(6)	O(9)−Ce(1)−O(13)	73.44(7)
O(1)−Ce(1)−O(14)	74.61(6)	O(1)−Ce(1)−O(6)	117.71(7)
O(2)−Ce(1)−O(8)	143.16(6)	O(2)−Ce(1)−O(7)	115.98(7)
O(6)−Ce(1)−O(9)	83.46(6)	O(8)−Ce(1)−O(13)	119.53(7)
O(7)−Ce(1)−O(13)	135.17(6)	O(9)−Ce(1)−O(14)	109.35(7)

Ce(IV)−Bis(5LIO-Me-3,2-HOPO) Complex, $[Ce(L^4)_2]\cdot 4H_2O$. This compound crystallizes from water in $P2_1/c$ with $Z = 4$. There is one metal complex and four crystalline water molecules in each asymmetric unit. The structure of $[Ce(L^4)_2]\cdot 4H_2O$ (with solvent) is shown in Figure 7, and selected bond lengths and angles are given in Table 5. The cerium is coordinated by eight oxygen atoms of the two 5LIO-Me-3,2-HOPO ligands with a sandwich-like shape. The top and bottom ligands are offset and rotated about 35° relative to one another (Figure 7), very different from that of about 133° in the $[Ce(L^4)_2]\cdot 2CH_3OH$ complex (Figure 6). It is notable that, in the structure of $[Ce(L^4)_2]\cdot 4H_2O$, there is extensive hydrogen bonding

Table 6. Protonation and Stability Constants for Bidentate and Tetradentate Me-3,2-HOPO Ligands and Their Ce(III) and Ce(IV) Complexes

	protonation		Ce(III) complexes					Ce(IV) complexes		
ligand	log K_1	log K_1K_2	logβ_{110}	logβ_{120}	logβ_{121}	logβ_{130}	logβ_{140}	logβ_{140}	logβ_{120}	pCe(IV)
HL^1	8.82(4)		6.07(8)	11.0(1)		14.6(2)				
HL^2	6.12(2)			11.12(7)		15.8(1)	19.7(1)	40.9(1)		25.9
H_2L^3	6.86(3)	12.8(1)		21.6(1)	24.9(1)				41.9(1)	37.5
H_2L^4	7.14(3)	13.05(1)	11.4(1)	20.9(2)	24.1(2)				40.6(2)	37.0

between the solvent (water) molecules as well the solvents and the complex molecules (Figure 7). Both O(2W) and O(3W) are hydrogen bonded to O(1W) and O(4W), respectively. O(1W) and O(4W) are hydrogen bonded to the HOPO amide oxygen O(3) and O(12) of one complex molecule and the HOPO amide oxygen O(10) and O(5) of another neighboring complex, respectively. In the structure of $[Ce(L^4)_2]\cdot 2CH_3OH$, there is no such extensive hydrogen-bonding network, and the complex takes a very different geometry.

The dihedral angle between the HOPO ring planes and their attached chelate planes (defined by the cerium and HOPO oxygen atoms) is 25.3°, very close to that in $[Ce(L^3)_2]\cdot 2CH_3OH$ (24.6°), but much larger than that in the methanol adduct $[Ce(L^4)_2]\cdot 2CH_3OH$ (13.3°), suggesting that the higher dihedral angles may be partially caused by the packing effect. Unlike the structure of $[Ce(L^4)_2]\cdot 2CH_3OH$, the coordination polyhedron of $[Ce(L^4)_2]\cdot 4H_2O$ is closest to a square antiprism (D_{4d}). The oxygen atoms within each of the square planes, O(1)O(2)O(6)O(7) and O(8)O(9)O(13)O(14), are coplanar; the mean deviations from the least-squares planes are 0.02 and 0.08 Å, respectively. The top and bottom square planes are essentially parallel, forming a dihedral angle of 4.8°. On the basis of shape analysis of all dihedral angles in $[Ce(L^4)_2]\cdot 4H_2O$, the calculated shape measures for different polyhedron geometries are

$$S(D_{2d}) = 20.7°; \quad S(C_{2v}) = 18.6°; \quad S(D_{4d}) = 12.5°$$

These values indicate that the coordination geometry of $[Ce(IV)(L^4)_2]\cdot 4H_2O$ can best be described as a square antiprism. Since the water and methanol adducts $[Ce(IV)(L^4)_2]\cdot 4H_2O$ and $[Ce(L^4)_2]\cdot 2CH_3OH$ differ only in the solvent of crystallization, the difference in shape between them is a dramatic example of the impact that solvent hydrogen bonding and crystal packing modes can have on the solid-state coordination geometry.

Solution Thermodynamics. Ligand Protonation Constants. The protonation constants of the HOPO ligands used in this work are listed in Table 6. The aqueous solubility of 5LI-Me-3,2-HOPO (H_2L^3) is at least 10 times lower than that of its oxygen analogue (H_2L^4), which strongly influenced the experiments carried out with the former ligand. The protonation constants of H_2L^3 are slightly lower than those of H_2L.[4] This may be due to additional intermolecular hydrogen bonds formed in solution between the HOPO protons and the oxygen atom in the chain.

Formation Constants of Bidentate Ce(III) Complexes with Me-3,2-HOPO Ligands. Not all of the formation constants of these complexes could be refined (Table 6), because of the relatively low solubility of the neutral 1:3 complexes and the gradual decrease in the stepwise stability constants. Despite the 500-fold difference in protonation constants between Me-3,2-HOPO (HL^1) and PR-Me-3,2-HOPO (HL^2), the values for the β_{120} constants of their Ce(III) complexes are equal within experimental error; the β_{130} values differ by only 1.2 log units. This suggests that the amide groups in HL^2 increase the complexation of Ce(III) by these two ligands via hydrogen bonding similar to that observed before in catecholamides.[32] Correlation coefficients between cumulative and the underlying stepwise formation constants[33] show that all parameters are independent ($R^2 < 0.2$).

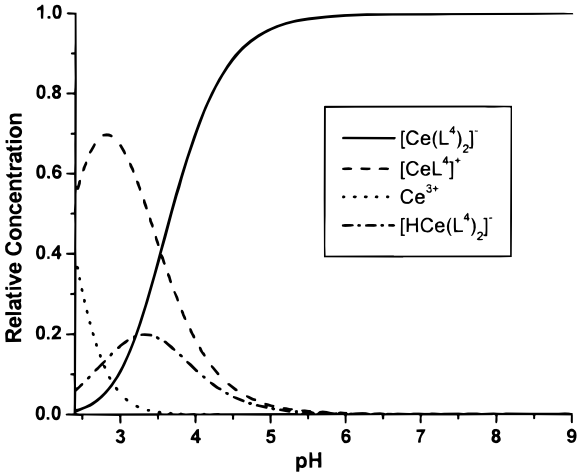

Figure 8. Relative species distribution in the Ce(III)−5LIO-Me-3,2-HOPO system at $[Ce^{3+}] = 100\ \mu M$ and [ligand] = 200 μM.

Formation Constants of Ce(III) Complexes with Tetradentate Me-3,2-HOPO Ligands. The potentiometric titrations of solutions with a 1:1 ratio of Ce(III) to H_2L^4 show evidence of hydrolysis at alkaline pH and cannot be fitted with a simple model. Information regarding the 1:1 complexes with H_2L^3 and H_2L^4 was, however, obtained independently from titrations in the 1:2 metal-to-ligand ratio. According to the calculations of species distribution (Figure 8), the 1:1 complex with H_2L^4 never dominates the distribution but is essential to the refinement. Since the 1:2 complexes are dominant near neutral pH (Figure 8), the β_{120} constants with Ce(III) are crucial for the determination of the corresponding stability constants with Ce(IV) (vide infra).

Formation Constants of Ce(IV) Complexes with Me-3,2-HOPO Ligands. Because of the oxidation of the ligands by Ce(IV) at low pH, no stability constant could be determined from *direct* potentiometric or spectrophotometric titrations alone, and no suitable competitor ligand with a well-known stability constant was available with which to perform a competition titration. Ultimately, a thermodynamic cycle was chosen to determine the log β_{1n0} values (Figure 9). The first step in the cycle requires the standard potential for the Ce(IV)/Ce(III) redox couple. The value of +1.70 V was used to calculate the corresponding $\Delta G°$.[34] The second step requires the β_{1n0} constants for the Ce(III) complexes. Finally, the standard potential for the reduction of the Ce(IV) complexes to the corresponding Ce(III) complexes was determined by static potential measurements or by cyclic voltammetry.

(32) Garret, T. M.; McMurry, T. J.; Hosseini, M. W.; Reyes, Z. E.; Hahn, F. E.; Raymond, K. N. *J. Am. Chem. Soc.* **1991**, *113*, 2965.
(33) Raymond, K. N.; McCormick, J. M. *J. Coord. Chem.* **1998**, *46*, 51.
(34) Hugus, Z. Z., Jr. University of California Radiation Laboratory Report 1379, July 9, 1951.

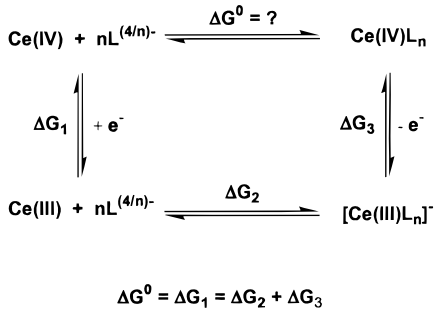

Figure 9. Thermodynamic cycle for the complexation of bidentate ($n = 4$) and tetradentate ($n = 2$) HOPO ligands with Ce(III) and Ce(IV).

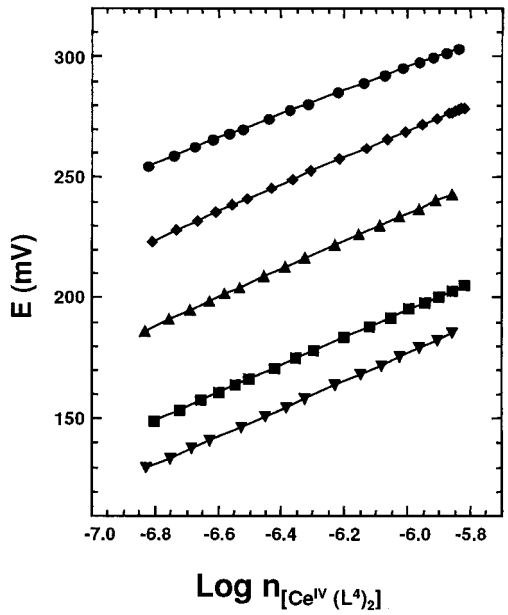

Figure 10. Static potential data for five different concentrations of $[Ce(III)(L^4)_2]$ as a function of the added molar amount of $[Ce(IV)(L^4)_2]$ in aqueous 0.1 M KCl. Key: (●) 0.462 μmol of Ce(III); (◆) 1.41 μmol of Ce(III); (▲) 5.21 μmol of Ce(III); (■) 25 μmol of Ce(III); (▼) 50.7 μmol of Ce(III).

Static Potentiometry. Figure 10 shows the potential from five data sets for the system containing $Ce(L^4)_2$ in water versus an AgCl/Ag half-cell. According to this experiment, the value of the standard potential (after correction with the value of 197 mV for the reference electrode)[35] equals +475 mV vs NHE, which corresponds to a potential drop for the Ce(IV)/Ce(III) couple of 1225 mV from its standard value. An even greater potential drop on the order of 2 V has been observed previously in the tetracatecholate complexes of Ce(IV) and Pu(IV).[13,14] Because of very low solubility in water, the static measurement determination of $E°$ for the Ce(IV)/Ce(III)−L^3 system had to be conducted in a mixed solvent by adding a solution of Ce(IV) complex in a minimal volume of DMF to an aqueous solution of its Ce(III) counterpart. Such an experiment was performed first with the Ce(IV)/Ce(III)−L^4 system to assess possible changes due to the presence of organic solvent. It was found that the intercept of the corresponding linear fit is higher by 8 mV, which can be explained by the complexation of Ce(III) with DMF.[36] Although the plot was linear ($R = 0.9997$), the 53.6 mV slope of the line was somewhat lower than the value of 59.1 mV expected for a one-electron process.

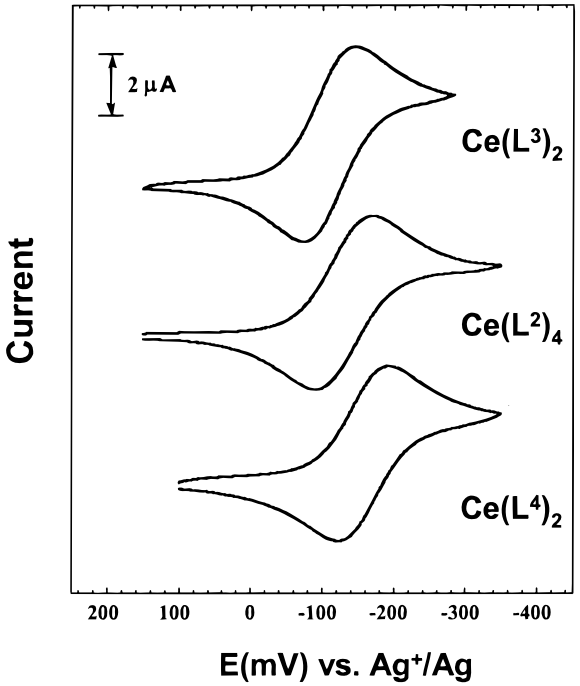

Figure 11. Cyclic voltammograms of cerium(IV) complexes with 3,2-HOPO ligands (0.5 mM complex solution on a glassy carbon electrode at a 20 mV/s scan rate; medium 0.1 M tetrabutylamonium hexafluorophosphate in acetonitrile).

The potential data for the Ce(IV)/Ce(III)−L^3 system were very similar though systematically higher: intercept of +306 mV vs AgCl/Ag (+503 mV vs NHE) and slope of 56.9 mV ($R = 0.9996$). The difference of 20 mV between the two intercepts translates into a difference of 0.33 log unit between the corresponding equilibrium constants.

The Ce−L^2 system did not exhibit reversible redox behavior at the concentration used, and the Ce−L^1 system showed no sensitivity to the addition of the Ce(IV) complex at neutral pH at all, presumably due to insufficient amounts of the corresponding $[Ce(III)(L)_4]^-$ complex at the given total concentration of the Ce(III) metal complex (0.5 mM) and the much higher stability of the Ce(IV) metal complex.

Cyclic Voltammetry. CV experiments for aqueous solutions of the Ce(III) complexes agreed with the results of the static measurements. The voltammograms of 1:2 complexes with H_2L^3 and H_2L^4 indicate reversible electrode kinetics (peak separation 70−80 mV, cathodic to anodic peak current ratio 0.80−0.95).[37] The peak separation was nearly 2 times larger for the 1:4 complex with HL^2, but decreased when excess ligand was added. This gave rise to a strong new anodic wave, attributed to ligand oxidation. The solution of Ce(III)−HL^1 (1:4) exhibited a clearly irreversible behavior.

In acetonitrile, three of the Ce(IV) complexes ($Ce(L^2)_4$, $Ce(L^3)_2$, and $Ce(L^4)_2$) gave clean reversible voltammograms (Figure 11). Solutions of the $Ce(L^1)_4$ complex, which is less stable, gave only irreversible voltammograms regardless of electrode choice and experimental conditions. Interestingly, the formal potentials in acetonitrile are in an entirely different order than in water. As for the static potentiometry results, the change of solvent is expected to affect the stability of the Ce(III)-

(35) Ives, D. J. G.; Janz, G. J. *Reference Electrodes*; Academic Press: New York, 1961.

(36) Tsibanov, V. V.; Bogatyrev, I. O.; Zaborenko, K. B. *Koord. Khim.* **1976**, *2* (2), 234.

(37) Bard, A. J.; Faulkner, L. R. *Electrochemical Methods*, Wiley: New York, 1980; pp 228−231.

containing species. A detailed understanding of this solvent effect would require knowledge of the solvation energies for both Ce(III) and Ce(IV) complexes and is beyond the scope of this investigation.

Spectrophotometric Titration. The formation of hydroxo-mixed complexes in the $Ce(IV)(L^3)_2$ and $Ce(IV)(L^4)_2$ systems (metal-to-ligand ratio 1:2) is manifested in the color change from purple to brown-yellow above pH 9. The equilibrium

$$Ce(IV)(L^4)_2 + OH^- \rightleftharpoons Ce(IV)(L^4)_2(OH)^- \qquad (2)$$

was investigated by spectrophotometric titration. An isosbestic point was observed near 500 nm in titrations from high to low pH, but its position was not the same in titrations in the reverse direction. Although significant bleaching seemed to occur at high pH, the solution remained clear with no visible formation of metal hydroxide precipitate. Because of these problems, only a tentative value of $\log K = -10.3(1)$ was obtained for this hydrolysis equilibrium constant.

Conclusions

The Me-3,2-HOPO ligands form very strong complexes with Ce(IV) in aqueous solution, giving overall formation constants ($\log \beta$) for $Ce(L^2)_4$, $Ce(L^3)_2$, and $Ce(L^4)_2$ of 40.9(1), 41.9(1), and 41.6(2), respectively. Because the deprotonation of these ligands is nearly complete at physiological pH, extraordinarily high pM values for Ce(IV) are obtained with the tetradentate ligands (37.5 for $Ce(L^3)_2$ and 37.0 for $Ce(L^4)_2$).

A criterion is suggested for evaluation of coordination geometry with regard to the degree to which it deviates from an ideal polyhedral shape. The proposed shape measure is the standard deviation (variance) of all dihedral angles (angles between normals of adjacent faces) from the idealized geometry, chosen from the Kepert model, $n = 8$.[28] Using this criterion, it is shown that the geometries deviate significantly from the idealized polytopal shape. The reported coordination geometries in the crystal structure were assigned to be best described as a trigonal dodecahedron in the case of $Ce(L^4)_2 \cdot 2CH_3OH$ and $Ce(L^1)_4 \cdot 2CH_3Cl$, and as a distorted square antiprism in the case of $Ce(L^4)_2 \cdot 4H_2O$. Small changes in the linear backbone of the tetradentate ligands and cocrystallized solvent molecules significantly affect the solid-state structures of their Ce(IV) complexes, while having little effect on the formation constants. Given that the complexation properties of Pu(IV) are very similar to those of Ce(IV),[12,13] these results suggest essentially the same structural and stability values for Pu(IV) and explain the great effectiveness of these ligands as plutonium sequestering agents *in vivo*.[6]

Acknowledgment. This research was supported by the Director, Office of Energy Research, Office of Basic Energy Sciences, Chemical Sciences Division, U.S. Department of Energy (DOE), under Contract Number DE-AC03-76SF00098 and the National Institute of Environmental Health Sciences Grant Number ES02698. Additionally, this research was supported in part under Grant No. SF17SP23, Environmental Management Science Program, Office of Science and Technology, Office of Environmental Management, U.S. DOE. M.Z thanks the Miller Foundation for a postdoctoral fellowship. We thank Drs. P. W. Durbin and D. Van Horn for helpful discussions and suggestions and Dr. F. J. Hollander for assistance with the X-ray diffraction studies.

Supporting Information Available: Listings of X-ray structural data for $[Ce(L^1)_4] \cdot 2CHCl_3$, $[Ce(L^3)_2] \cdot 2CH_3OH$, $[Ce(L^4)_2] \cdot 2CH_3OH$, and $[Ce(L^4)_2] \cdot 4H_2O$ including a summary of crystallographic parameters, atomic coordinates, bond distances and angles, and anisotropic thermal parameters as well as the computer program to calculate the "shape measure". This material is available free of charge via the Internet at http://pubs.acs.org. Crystallographic data (excluding structure factors) for the structures reported in this paper have been deposited with the Cambridge Crystallographic Data Center as supplementary publication nos. CCDC-121635, -121626, -121637, and -161238. Copies of the data can be obtained free of charge on application to CCDC, 12 Union Rd., Cambridge CB21EZ, U.K. (fax (+44) 1223-336-033; e-mail deposit@ccdc.camac.uk).

IC000063I